pp. 1–15 (2017)

Mathematical modelling of chemotherapy combined with bevacizumab

M. B. Kuznetsov* and A. V. Kolobov*

Abstract — Antiangiogenic therapy is aimed at the blocking of angiogenesis, i.e., the process of new blood vessels formation, which should decrease oxygen and nutrients inflow to tumor and thus slow down its growth. This type of therapy is frequently administered together with chemotherapy, which kills rapidly proliferating tumor cells, as well as other dividing cells of the body, thus leading to significant adverse effects. However, action of bevacizumab inevitably influences the inflow of chemotherapeutic drug in tumor, therefore, optimal scheduling of drug administration is an important problem. Using a model based on consideration of the most crucial processes happening during tumor progression and therapy, we compare effectiveness of different schemes of combined chemotherapy with bevacizumab and propose new scheme of drug administration which may lead to enhanced antitumor effect compared to classical clinical scheme of simultaneous drug administration.

Keywords: Tumor modelling, chemotherapy, antiangiogenic therapy, bevacizumab.

MSC 2010: 92B99

After many years of cancer research, it has been widely accepted that tumors are complex tissues consisting of many components interacting with each other rather than merely colonies of malignant cells [16]. Despite all the incredible diversity of tumor types, every single tumor contains normal tissue compartment, which is actively participating in the process of tumor progression. Therefore, normal cells in tumor tissue along with the signaling pathways which interconnect them with malignant cells have also been recognized as potential targets to therapeutic interventions. A distinguished example of this type of treatment is antiangiogenic therapy, which is aimed at the blocking of angiogenesis, i.e., the process of new blood vessels formation. This type of therapy was suggested in 1971 by Folkman [11]. The first antiangiogenic drug, bevacizumab, was approved for medical use in 2004 and is widely used nowadays.

Pre-existing vascular system limits the rate of tumor growth. Tumor cells often require larger oxygen and metabolites supply than normal cells; blood capillaries inside the tumor can degrade by various chemical and mechanical reasons; moreover, proliferating tumor tissue extrudes surrounding tissues with their vessels, moving away metabolite sources from its main mass. This limitation is overcome by tumor neovascularization, governed by tumor-induced proangiogenic factors, of

*P. N. Lebedev Physical Institute of the Russian Academy of Sciences. 53 Leninskii Prospekt, Moscow 119991, Russia. E-mail: kuznetsovmb@mail.ru

The research was supported by the RSF grant 14-31-00024.

which vascular endothelial growth factor, or VEGF, is accepted to be the most important one. However, due to overproduction of proangiogenic factors by tumors, their newly formed microvasculatory system is chaotic and the capillaries themselves are dilated, tortuous, and highly permeable [2]. The action of VEGF can be inhibited by neutralizing it or its signaling pathways in endothelial cells, e.g., bevacizumab binds irreversibly to VEGF, rendering it inactive. Antiangiogenic therapy leads to capillaries maturation and prevents the formation of new capillaries thus depriving tumor of nutrients and decelerating its growth. Compared to traditional radio- and chemotherapy, antiangiogenic therapy has moderate side-effects, but it alone can not eradicate tumor, so it is reasonable to administer it together with another therapy aimed at the direct tumor cells killing. Due to this, nowadays almost all of the approved administration schemes, which include bevacizumab, combine it with various chemotherapy agents [12], the main aim of which is intervention in the process of cell division. The action of these agents is not specific to cell types, but as tumor cells divide much more frequently than normal ones, impact of chemotherapy on them prevails over effect on surrounding normal cells. Nevertheless, this kind of therapy often leads to significant side-effects, such as anemia, hair loss, mucositis and nausea.

Two different types of antitumor drugs, administered simultaneously, inevitably interact with each other in different ways, e.g., chemotherapy slows down neovascularization rate by interfering with division of endothelial cells, thus enhancing antiangiogenic action [19]. On the other hand, maturation of tumor capillaries resulting in decrease in their permeability and their subsequent degradation due to antiangiogenic therapy lead to reduced influx of chemotherapeutic drug in tumor, which was observed experimentally [5, 25]. Therefore, a great challenge concerning cytotoxic chemotherapy combined with antiangiogenic agent is the problem of optimal scheduling of drugs administration in order to maximize antitumor effect and minimize side-effects. The topic is being actively investigated now, and mathematical modelling can facilitate its investigation.

At present, in contrast to clinical practice, the mathematical modelling of combined antitumor chemotherapy with antiangiogenic agents is only at its early stage [1, 15]. In fact, all existing works of this type do not take into account the spatial structure of the tumor, which indicates that they are only suitable for the simulation of postoperative (adjuvant) therapy. Moreover, the effect of antiangiogenic drugs is described only phenomenologically in these models. However, there are a lot of works on classical chemotherapy modelling [6, 10, 27], from which modelling approaches and reference parameters of common drugs may be used. Furthermore, the modelling of bevacizumab pharmacodynamics in blood and tissue as application to cancer [4, 23] and ophthalmic diseases [21] has already begun.

An important factor requiring detailed consideration is the fact that standard chemotherapeutic agents, such as doxorubicin, cisplatin, oxoplatinum, have low molecular weight (a few hundred Daltons) unlike macromolecular bevacizumab (149 kDa) and VEGF (about 40 kDa). Thus, during the modelling of their pharmacodynamics in blood and tissue, it is necessary to take into account the mechanisms

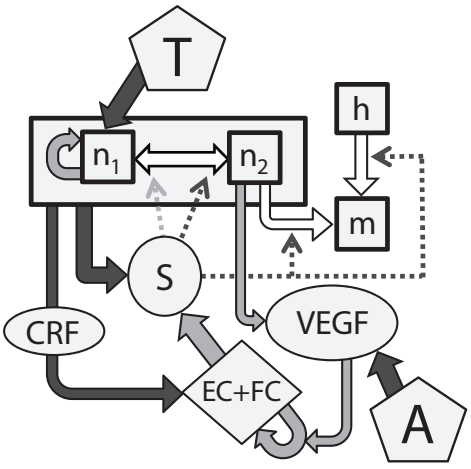

Figure 1. Block-scheme of the model of tumor progression and combined antitumor chemotherapy with bevacizumab. n_1 and n_2 are proliferating and migrating tumor cells respectively, h are host cells, m is necrosis, S is glucose, $VEGF$ is vascular endothelial growth factor, EC and FC are preexisting and angiogenic microcirculatory networks respectively, CRF is capillary regression factors, A is bevacizumab, T is chemotherapy agent. Gray arrows indicate stimulating relations, black arrows indicate inhibiting relations, white arrows denote cell transitions.

of their non-specific binding, the rate of which highly depends on patient-specific characteristics, tumor localization and various other factors. This introduces a large portion of uncertainty in determination of model parameters.

In this work we compare the effectiveness of different schemes of palliative combined chemotherapy with bevacizumab. Unlike neoadjuvant therapy, which is held before surgery and consists of 4-6 drug injections, palliative therapy takes place when surgical intervention is not possible, and administration of drugs continues until tumor remission or lethal outcome.

1. Model

Figure 1 demonstrates the block-scheme of the model under investigation. We rely on widely-accepted principle of migration/proliferation dichotomy of tumor cells, according to which a tumor cell can not actively move and divide simultaneously [14], and therefore we consider heterogeneous colony of living tumor cells: proliferating ones, normalized density of which is $n_1(r,t)$, and migrating ones, which density is $n_2(r,t)$, where r and t are space and time coordinates. Each malignant cell can change its state depending on the level of glucose, which is selected as the key metabolite, its concentration is $S(r,t)$. Tumor grows in a tissue consisting of normal cells with density $h(r,t)$. When dying, tumor and normal cells form necrosis, whose fraction in tissue is $m(r,t)$. In absence of tumor, the tissue contains preexisting normal capillary network, the bulk density of its surface is $EC(r,t)$. As a result of tumor neovascularization, the microcirculatory network expands by angiogenic capillaries, their surface bulk density is $FC(r,t)$. This variable is included in the model to account for the fact that permeability of angiogenic capillaries is higher than that of normal capillaries, due to the presence of large pores, i.e., fenestrations, in their walls [24]. Furthermore, as a result of tumor progression microcirculatory network locally degrades under the influence of several factors – mechanical ones, such as vascular occlusion due to swelling of the tumor, and chemical ones, an

example of which is angiopoietin-2, which is produced by endothelial cells themselves in the tumor microenvironment [17]. We do not consider in details relevant biochemical processes, but introduce a new variable $CRF(r,t)$, which determines the regression of capillaries. The model also takes into account concentrations of vascular endothelial growth factor, or VEGF, $V(r,t)$ and antiangiogenic drug bevacizumab $A(r,t)$, which irreversibly binds to it, thereby blocking tumor angiogenesis. Concentration of chemotherapeutic agent $T(r,t)$ is included as well, its action directly leads to death of dividing tumor cells.

Equations describing the densities of cell populations and concentration of necrosis are as follows:

$$\begin{aligned}
\frac{\partial n_1}{\partial t} &= Bn_1 - P_1(S)n_1 + P_2(S)n_2 - (k_{n1}T_n)Tn_1 - \nabla(In_1)\\
\frac{\partial n_2}{\partial t} &= D_n\Delta n_2 + P_1(S)n_1 - P_2(S)n_2 - d_n(S)n_2 - \nabla(In_2)\\
\frac{\partial h}{\partial t} &= -d_h(S)h - \nabla(Ih)\\
\frac{\partial m}{\partial t} &= d_n(S)n_2 + d_h(S)h + (k_{n1}T_n)Tn_1 - \nabla(Im)\\
P_1(S) &= k_1\exp(-k_2S)\\
P_2(S) &= \frac{1}{2}k_3(1-\tanh[\varepsilon_{\text{trans}}(S_{\text{trans}}-S)])\\
d_n(S) &= \frac{1}{2}d_{n,\max}(1+\tanh[\varepsilon_{\text{cells}}(S_{\text{crit}}-S)])\\
d_h(S) &= \frac{1}{2}d_{h,\max}(1+\tanh[\varepsilon_{\text{cells}}(S_{\text{crit}}-S)])\\
n_1+n_2+m+h &= 1, \qquad \nabla I = Bn_1 + D_n\Delta n_2.
\end{aligned} \tag{1.1}$$

At any moment of time each tumor cell either proliferates at the rate B or randomly moves with the diffusion coefficient D_n, the intensities of transitions from one state to another are $P_1(S)$ and $P_2(S)$, respectively, depending on the concentration of glucose. The forms of these functions are described in detail in our previous work [23]. Both tumor and host cells die due to lack of glucose with rates $d_n(S)$ and $d_h(S)$, respectively. They can also die in result of chemotherapy. All dying cells turn into necrosis. The effectiveness of the chemotherapeutic drug, regardless of the details of its mechanism of action, is described by the parameter k_{n1}, which governs the rate of proliferating cells death. The concentration of the drug in blood is normalized to its dosage T_n.

We consider an incompressible dense tissue in which space distribution of tissue components is affected by their local kinetics, e.g., dividing cells push out surrounding tissues, providing an increase of tumor size. To account for these effects, we introduce the convective flows field $I(r,t)$, which in general case is derived the following way.

Consider a system of equations for the subpopulations of cells n_i, which can divide, die, transform into each other, and also possess intrinsic mobility, while the total cell density is constant and equal to unity. For simplicity, the volumes of all the cells are equal. The evolution of the system is described by the equations:

$$\frac{\partial n_i}{\partial t} = f_i(\mathbf{n},\cdot) + D_i \Delta n_i - \nabla(n_i \mathbf{I}).$$

Here $f_i(\mathbf{n},\cdot)$ are the functions that describe the local kinetics of cell populations, depending on densities of cells themselves and on external conditions; D_i is the diffusivity of cells of i-th population, $\mathbf{I}$ is the velocity of convective motion, the gradient of which can be expressed by summing up left and right sides of equations:

$$\nabla \mathbf{I} = \sum_i [f_i(\mathbf{n},\cdot) + D_i \Delta n_i]$$

the terms of cell transitions being mutually canceled out. In the case considered herein, local cell kinetics comprises division of cells in population n_1 and diffusion of cells in population n_2, which results in the formula for convective flow velocity field (see (1.1)).

As already mentioned, the model uses two variables to describe the vascular network – EC and FC, which are the surface densities of normal and angiogenic capillaries, the latter having significantly higher permeability. Equations describing the dynamics of capillary surface density are as follows:

$$\begin{aligned}
\frac{\partial EC}{\partial t} =& -\mu(EC+FC-1)EC\cdot\Theta(EC+FC-1) - k_{CRF}CRF\cdot EC \\
& - l(n_1+n_2)EC + v_{\text{mat}}FC\cdot \mathrm{e}^{-V/V_{\text{norm}}} - \nabla(\text{elast}\cdot I\cdot EC) \\
\frac{\partial FC}{\partial t} =& D_{FC}\Delta FC + R\mathrm{e}^{-T/T_{Re}}\Theta(S-S_{\text{crit}})\frac{V}{V+V^*}(EC+FC) \\
& - \mu(EC+FC-1)FC\cdot\Theta(EC+FC-1) - k_{CRF}CRF\cdot FC \\
& - l(n_1+n_2)FC - v_{\text{mat}}FC\cdot \mathrm{e}^{-V/V_{\text{norm}}} - \nabla(\text{elast}\cdot I\cdot FC)
\end{aligned} \tag{1.2}$$

where μ is the parameter responsible for the microcirculatory network tendency to return to constant physiologically reasonable density due to decrease blood filling in capillaries with the increase in microcirculatory network density above physiologically reasonable level; k_{CRF} is the rate of capillaries destruction caused by chemical factors; l is the parameter of capillaries degradation under mechanical pressure; R is the maximum rate of angiogenesis achieved at high concentrations of VEGF and sufficient concentrations of glucose in the absence of chemotherapy, which slows down the division of endothelial cells. Parameter v_{mat} is responsible for maturation of angiogenic capillaries in absence of VEGF. Dynamics of microcirculatory network is described by random movement of angiogenic capillaries with the coefficient of diffusion D_{FC} and by convective motion of the entire network at the speed

of elast$\cdot I$, which is less than the speed of convective cell movement due to microcirculatory network connectivity.

Change of glucose concentration S is defined by the equation:

$$\frac{\partial S}{\partial t} = D_S \Delta S + [P_{S,EC} EC + P_{S,FC} FC](S_{\text{blood}} - S) - [q_{n1} n_1 + q_{n2} n_2 + q_h h] \frac{S}{S + S^*}. \tag{1.3}$$

Here D_S is the diffusion coefficient of glucose in tissue; its uptake rate by different cells is designated by letters q with corresponding indices; glucose inflow from capillaries of both types is characterized by parameters $P_{S,EC}$ and $P_{S,FC}$, S_{blood} is the blood level of glucose, which is considered to be constant.

Balance of capillary regression factors CRF is set by the following expression, terms of which designate respectively their diffusion, production by tumor cells, utilization as the result of interaction with microcirculatory network and non-specific degradation:

$$\frac{\partial CRF}{\partial t} = D_{CRF} \Delta CRF + p_{CRF}(n_1 + n_2) - \omega_{CRF} CRF\,(EC + FC) - d_{CRF} CRF. \tag{1.4}$$

Equations determining the concentrations of VEGF, bevacizumab and chemotherapy agent are as follows:

$$\begin{aligned}
\frac{\partial V}{\partial t} &= D_V \Delta V + p_V n_2 - \omega_V V (EC + FC) - d_V V - (k_A A_n) AV \\
\frac{\partial A}{\partial t} &= D_A \Delta A + [P_{A,EC} EC + P_{A,FC} FC](A_{\text{blood}} - A) - (k_A V_n) AV \\
\frac{\partial A_{\text{blood}}}{\partial t} &= F_{A,iv} - d_A A_{\text{blood}} \\
\frac{\partial T}{\partial t} &= D_T \Delta T + [P_{T,EC} EC + P_{T,FC} FC](T_{\text{blood}} - T) - d_{T,\text{tissue}} T \\
\frac{\partial T_{\text{blood}}}{\partial t} &= F_{T,iv} - d_{T,\text{blood}} T.
\end{aligned} \tag{1.5}$$

Here D_V, D_A, and D_T are the diffusivities of corresponding substances, p_V is the production rate of VEGF by migrating tumor cells, which are in a state of metabolic stress, ω_V is the rate of VEGF binding to endothelial cells receptors, d_V is the rate of its non-specific degradation. Irreversible binding of bevacizumab to VEGF is characterized by the constant k_A. Capillary permeabilities for drugs are designated by letters P with corresponding indices. Coefficients A_{blood} and T_{blood} are the blood levels of drugs, their administration schemes are described by functions $F_{A,iv}$ and $F_{T,iv}$, while d_A and $d_{T,blood}$ are the rates of drugs elimination from blood, $d_{T,\text{tissue}}$ is the rate of non-specific binding of chemotherapeutic agent.

2. Results

The set of equations (1.1)–(1.5) was solved in one-dimensional region with size of $L = 3$ *cm*. Numerous experimental studies demonstrate that when tumor radius is

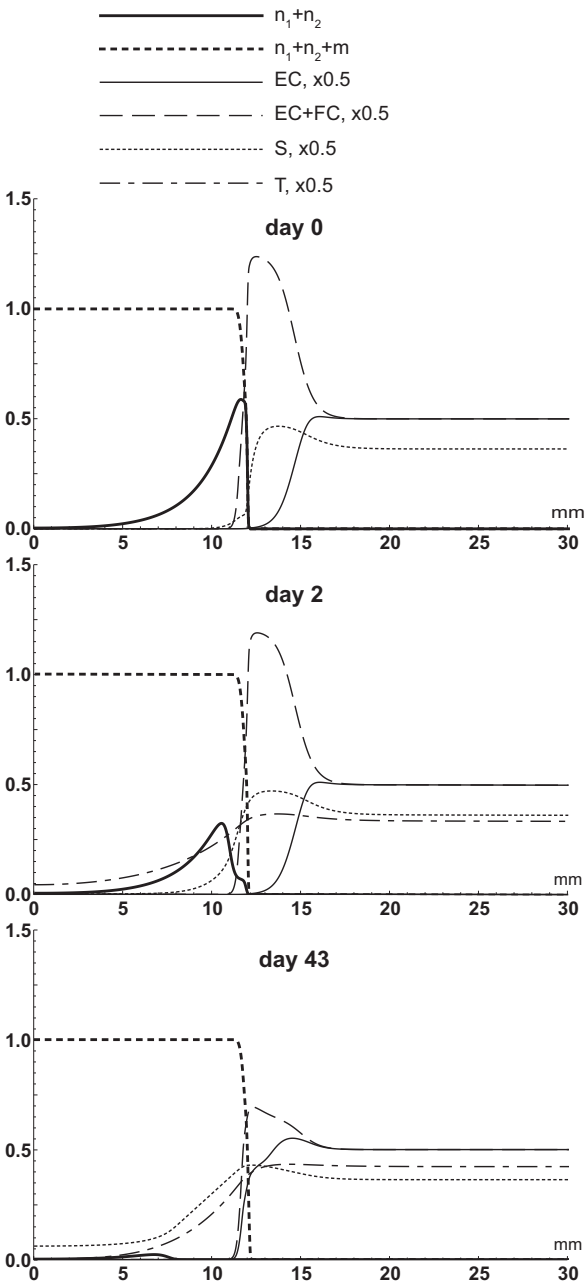

Figure 2. Profiles of living tumor cells density $n_1 + n_2$, fraction of tumor with necrosis $n_1 + n_2 + m$, normal microcirculatory network surface density EC, total microcirculatory network surface density $EC + FC$, concentrations of glucose S and chemotherapeutic agent T on the day before the start of chemotherapy and on the 2nd and 43th days of its administration under the drug effectiveness $k_{n1} = 4.6 \times 10^7$.

more than several millimeters, its center is occupied by necrotic core. Therefore using of plane geometry does not lead to the significant deviations of results compared to spherically symmetric problem, since the Laplace operators in these cases differ significantly only for small radii. Initially we place a colony of tumor cells on the left border, which represents tumor center. For all variables zero-flux boundary conditions were set on both borders. The convective flow speed was set zero on the left border, free boundary condition was used for it on the right border. All parameters of the model were non-dimensionalized, the following normalization values were selected for: time – $t_n = 1\ h$, length – $L_n = 10^{-2}\ cm$, concentration of glucose – $S_n = 1$ mg/ml, concentration of VEGF – $V_n = 10^{-11}$ mol/ml, concentration of bevacizumab – $A_n = 10^{-9}$ mol/ml, concentration of chemotherapeutic agent – $T_n = 4.1 \times 10^{-8}$ mol/ml. Maximum cell density was set as $n_{\max} = 10^9$ cells/ml, normal capillary surface density was set as $EC_n = 50\,\mathrm{cm}^{-1}$ [33]. Microcirculatory network initially consists only of normal body capillaries, so $EC(x,0) = 1$. The initial distribution of glucose $S(x,0)$ depends on the system parameters and is calculated as the steady-state concentration of glucose in normal tissue without tumor, $n_1(x,0) = max(0, 0.25(1 - [x^2/100]))$, which puts small (1 mm in width) population of proliferating tumor cells near the left boundary. The other variables at the initial time moment are equal to zero.

To speed up the calculations, equations for VEGF, oxygen and glucose were considered in the quasi-stationary approximation due to high rates of their reactions with respect to these rates for other variables and were solved numerically using the tridiagonal matrix algorithm. For other variables, the method of splitting into physical processes was used. Kinetic equations were solved via the fourth-order Runge–Kutta method and Crank–Nicholson scheme was used for the diffusion equations. Convective equations were solved using the flux-corrected transport algorithm [3] with the use of explicit anti-diffusion stage.

The following parameters were chosen as the basic set:

$$
\begin{array}{lll}
B = 0.01, & D_n = 0.0036, & k_1 = 0.4\ [32] \\
k_2 = 19.8\ [32], & k_3 = 0.08, & \varepsilon_{\text{trans}} = 10\ [32] \\
S_{\text{trans}} = 0.3\ [32], & d_{n,\max} = 0.0005, & S_{\text{crit}} = 0.1 \\
d_{h,\max} = 0.02, & \varepsilon_{\text{cells}} = 5, & \mu = 0.001 \\
k_{CRF} = 5 \times 10^{-5}, & l = 0.0025, & v_{\text{mat}} = 0.0025 \\
V_{\text{norm}} = 0.025, & \text{elast} = 0.5, & R = 0.0015 \\
T_{Re} = 0.07, & V^* = 0.1, & D_{FC} = 0.00036 \\
q_{n1} = 500, & q_{n2} = 3.125, & q_h = 3.125 \\
S^* = 0.02\ [32], & P_{S,EC} = 2, & P_{S,FC} = 4.8 \\
S_{\text{blood}} = 1, & D_S = 180\ [13], & p_{CRF} = 100 \\
\omega_{CRF} = 0.5, & d_{CRF} = 0.05, & D_{CRF} = 21.6 \\
p_V = 200\ [20], & \omega_V = 0.23, & d_V = 0.46\ [22] \\
k_A = 1.9 \times 10^{12}\ [30], & D_V = 21.6\ [26], & P_{A,EC} = 0.002 \\
P_{A,FC} = 1.23, & D_A = 7.2\ [12], & d_A = 0.0014\ [12] \\
P_{T,EC} = 1, & P_{T,FC} = 2.75, & D_T = 120 \\
d_{T,\text{blood}} = 0.01, & d_{T,\text{tissue}} = 0.14. &
\end{array}
\tag{2.1}
$$

The rate of tumor cell proliferation approximately corresponds to one division in three days, their diffusion coefficient corresponds to non-diffuse tumor. Parameter μ is chosen so that microcirculatory network can not become more than two and a half times denser. Proliferating tumor cells require much more glucose than the others, since it is a basic plastic substrate. Parameters of permeability of both types of capillaries for glucose and drugs are evaluated using Renkin equation, it was done in the same way in [23]. For the sake of simplicity, we assume that chemotherapeutic agent does not bind with blood proteins.

To describe the chemotherapeutic agent, parameters of cisplatin were used [27, 36] as it is one of the most commonly used chemotherapeutic drugs in combination with bevacizumab [35, 38]. The drug toxicity parameter k_{n1} varies for the investigation of therapy effectiveness. Cisplatin administration scheme in clinical practice is every time selected based on the specific situation, we simulate six drug injections at three-week intervals. The injection of drug implies an increase of value of its blood concentration variable T_{blood} by one, drug dosage being defined by its normalization constant T_n.

Figure 2 demonstrates the distribution of model variables during cytotoxic monochemotherapy under drug effectiveness $k_{n1} = 4.6 \times 10^7$. The top picture shows the profiles of malignant cells, microcirculatory network and glucose on the day before the start of therapy. Increased glucose concentration in the peritumoral area, where active angiogenic capillaries formation takes place, infers its greater inflow in this area. Angiogenesis also influences the inflow of chemotherapeutic agent, the permeability ratio of angiogenic and preexisting capillaries for it being slightly higher than that for glucose, since drug molecules are larger. Proliferating tumor cells are concentrated near the tumor boundary (in the area with sufficiently high glucose concentration for proliferation) and middle picture shows how their number reduces significantly on the second day after the first injection of the drug. In result of death of these cells, depth of glucose penetration into the tumor increases that leads to active transition of migrating cells n_2 into proliferating state in which they are also killed by the action of chemotherapeutic drug. The bottom figure illustrates the 43-rd day of therapy to which the number of viable tumor cells is significantly reduced, while the remaining cells are concentrated in depth of the tumor. Normalization of angiogenic capillaries results in decrease in effective permeability of microcirculatory network, while action of various chemical and mechanical factors leads to significant decrease of its overall density. Both factors affect the decrease in inflows of drug and glucose to the tumor.

Figure 3 demonstrates the dynamics of change in the number of living tumor cells with time for different effectiveness of chemotherapeutic agent k_{n1}. The drug with effectiveness $k_{n1} = 4.6 \times 10^4$ has no significant effect on the dynamics of tumor growth which would be distinguishable on this graph, under $k_{n1} = 4.6 \times 10^5$ tumor volume slightly decreases during the therapy, but after it number of cells quickly recovers, under $k_{n1} = 4.6 \times 10^6$ it becomes possible to achieve significant long-term reduction in the number of tumor cells, under $k_{n1} = 4.6 \times 10^7$ in the middle of therapy course the number of tumor cells decreases critically, under $k_{n1} = 4.6 \times 10^8$

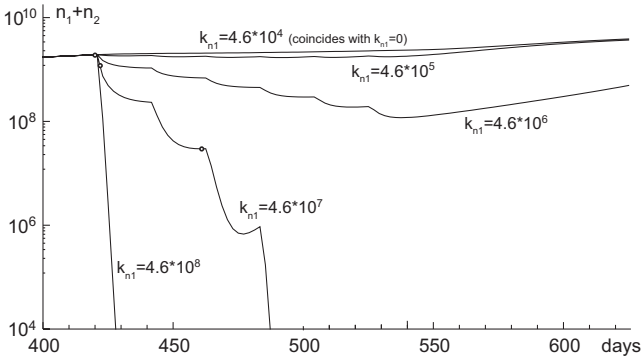

Figure 3. The number of tumor cells $n_1 + n_2$ during chemotherapy depending on the drug effectiveness k_{n1}. Points denote moments in time for which the variables profiles are shown in 2 under drug effectiveness value of $k_{n1} = 4.6 \times 10^7$.

practically all tumor cells die already after the first injection. For the case $k_{n1} = 4.6 \times 10^7$ the points on the graph denote the time moments, for which Figure 2 shows the distributions of model variables.

There was conducted an investigation of relative effectiveness of various schemes of drug administration during combination therapy. In each scheme chemotherapeutic agent is administered six times with three-week intervals. In the first scheme the antiangiogenic drug bevacizumab is not used at all, so monochemotherapy is modelled. In the second scheme, which is used commonly in clinical practice, bevacizumab is injected at the same time with chemotherapeutic agent, starting from its first injection, and administration of bevacizumab continues after the end of chemotherapy. The third scheme differs from the second in that the bevacizumab is administered only from the sixth injection of the chemotherapeutic drug. The comparison of the schemes effectiveness was made under different values of non-specific binding of chemotherapeutic drug in tissue $d_{T,\text{tissue}}$, as it is an important parameter which in practice can vary significantly depending on the characteristics of patient and tumor and various other factors. The smaller its value, the less chemotherapeutic agent binds to tumor microenvironment elements and the more deeply the drug penetrates into the tumor. Figure 4 shows the dynamics of tumor cells number under three different values of $d_{T,\text{tissue}}$ for three schemes of drug administration.

It is seen from Fig. 4 that the rate of non-specific binding of chemotherapeutic drug heavily influences the therapy effectiveness, but the scheme of simultaneous drugs administration, widely used in clinical practice, turns out to be not the best one in a wide range of values $d_{T,\text{tissue}}$. Scheme with bevacizumab administration starting at the end of chemotherapy is more effective.

To quantify the effectiveness of therapy the time of tumor remission can be used, which we conditionally defined as the number of days during which the number of tumor cells is not more than 10^6. Under $d_{T,\text{tissue}} = 0.028$ the delay in bevacizumab administration increases this parameter from 828 to 843, that is, by 2%, under $d_{T,\text{tissue}} = 0.14$ – from 257 to 299, that is, by 16%. This result is explained by the fact that the administration of bevacizumab from the very beginning of the

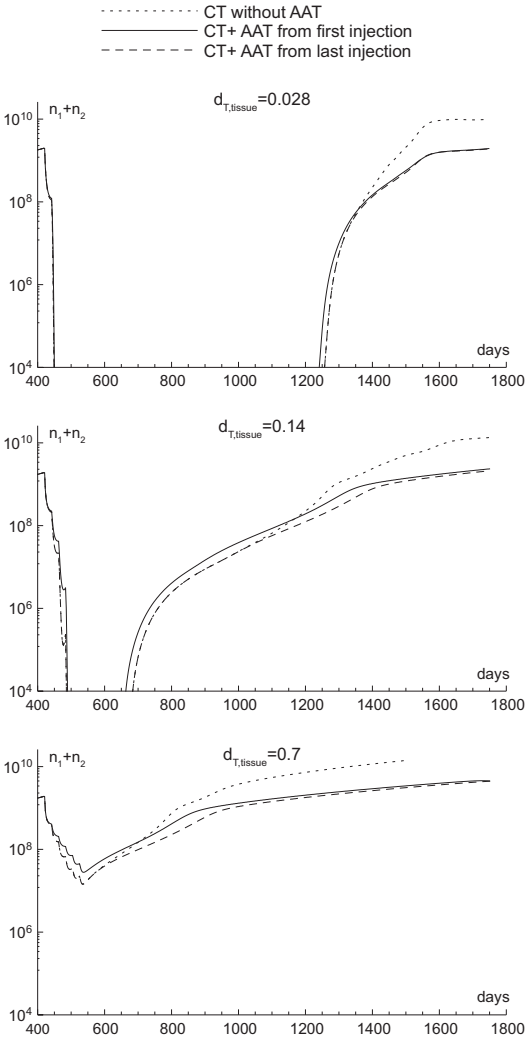

Figure 4. The number of tumor cells during combined chemotherapy with antiangiogenic drug under chemotherapeutic drug effectiveness value of $k_{n1} = 5 \times 10^7$ at different values of the rate of its non-specific binding $d_{T,\text{tissue}}$. CT – chemotherapy, AAT – antiangiogenic therapy.

combined therapy leads to rapid maturation of capillaries formed in result of tumor angiogenesis and their later degradation – this significantly reduces the effective capillary permeability for chemotherapeutic drug and consequently fewer tumor cells are killed by it.

3. Discussion

In this work, basing on the results of mathematical simulations it was suggested that scheduling of combined chemotherapy with bevacizumab when administration of

the latter begins with the end of chemotherapy should lead to enhanced antitumor effect compared to classical clinical scheme of simultaneous drug administration. The main reason of this is that more chemotherapeutic drug should flow in tumor tissue through angiogenic capillaries than through normal and maturated ones due to their greater permeability. This result is of purely qualitative nature, and its quantitative pre-estimation in every specific experimental or clinical case is a hardly feasible task, since it depends on colossal number of parameters of different nature. Nevertheless, this result is based on the consideration of the most crucial processes taking place during tumor progression and therapy, and therefore is of great potential practical importance and has to be checked by direct experiments. It should be specially noted that estimation of tumor angiogenic capillaries permeability for chemotherapeutic drug has been made herein for certain parameter values and with neglecting the fraction of drug molecules reversibly bound to plasma proteins. For instance, plasma protein binding for cisplatin is estimated as 95% [34], however, plasma proteins molecular masses can be two orders of magnitude more than that of cisplatin itself, so permeability for such complexes through pre-existing or maturated capillaries is negligible compared to that of free drug. Thus, the model overestimates overall drug inflow during antiangiogenic treatment, and more detailed consideration of drug pharmacokinetics would only enhance the effectiveness of introduced scheme compared to simultaneous drug administration.

Nowadays the majority of experimental investigations aimed at optimization of combined chemotherapy with bevacizumab focus on the concept, which appeared in the beginning of this century and has gained wide interest [18]. It was proposed that right after beginning of antiangiogenic therapy there exists a transient period of ‘normalization window’ when tumor gets enhanced supply of oxygen, nutrients and drugs, and this happens due to the fact that tumor capillaries prior to their degradation become mature which leads to increased tumor blood flow. Experimental investigations on various mice tumor models indeed demonstrated elevated levels of oxygen concentration in tumor tissue lasting several days after beginning of antiangiogenic therapy. Consequently, combined radiation and antiangiogenic therapy had synergistic effect when the former was administered during the ‘normalization window’ [9,28], as the effect of radiation therapy strongly depends on the formation of reactive oxygen species, which interfere with cell division.

However, according to existing experimental data on changes of tumor blood perfusion, during first days after antiangiogenic therapy, in different cases it can either increase [8] or decrease [29, 37]. Moreover, rate of oxygen consumption by tumor can be also strongly affected by antiangiogenic therapy [7]. These and other data raise certain questions on boundaries of applicability and correct theoretic explanation of the effect of ‘normalization window’.

Most importantly, since the inflow of the majority of metabolites and drugs is mainly governed by the diffusion process through the capillary membrane [24], increased tumor blood perfusion alone should elevate chemotherapy agent influx in tumor only in cases of severely impaired tumor blood perfusion before treatment, otherwise it should not affect drug influx significantly. Indeed, injection of bevaci-

zumab results in rapid sustained decrease of effective tumor capillaries permeability for lipid-insoluble molecules, to the class of which chemotherapeutic agents also belong, which was unambiguously demonstrated by numerous experiments, including above mentioned ones [8,28]. Still, even in the cases when appearance of 'normalization window' would influence the chemotherapeutic drug inflow, this effect would be very limited in time, and would affect only one injection of drug, after which due to degradation of tumor microvasculature drug inflow in tumor would unavoidably be severely limited. On the contrary, combined therapy scheduling suggested herein would take advantage of increased capillary permeability for the whole course of chemotherapy administration and therefore should integrally be more effective. To the best of our knowledge, by now there has been no direct experiment held that would have compared the suggested scheme with simultaneous administration.

In the present paper, only palliative therapy was considered. Investigation of neoadjuvant therapy effectiveness should rely on the rate of decrease of tumor radius, since it is the main clinically relevant parameter. The model herein cannot reproduce tumor shrinkage, since it does not consider interstitial fluid dynamics. Thus, it can not describe fluid outflow from necrotic into peritumoral area and then into lymphatic system which leads to tumor volume decrease observed as a result of neoadjuvant chemotherapy. Therefore to carry out such investigation it is necessary to expand the existing model, taking into account the dynamics of interstitial fluid.

References

1. S. Benzekry, G. Chapuisat, J. Ciccolini, A. Erlinger, and F. Hubert, A new mathematical model for optimizing the combination between antiangiogenic and cytotoxic drugs in oncology. *Comptes Rendus Mathematique* **350** (2012), No. 1, 23–28.
2. G. Bergers and E. B. Laura, Tumorigenesis and the angiogenic switch. *Nature Reviews Cancer* **3** (2003), No. 6, 401–410.
3. J. P. Boris and D. L. Book, Flux-corrected transport, I. SHASTA, a fluid transport algorithm that works. *J. Comp. Phys.* **11** (1973), No. 1, 38–69.
4. J. Chen, B. Liu, J. Yuan, J. Yang, J. Zhang, Y. An, L. Tie, Y. Pan, and X. Li, Atorvastatin reduces vascular endothelial growth factor (VEGF) expression in human non-small cell lung carcinomas (NSCLCs) via inhibition of reactive oxygen species (ROS) production. *Molecular Oncology* **6** (2012), No. 1, 62–72.
5. A. Claes, P. Wesseling, J. Jeuken, C. Maass, A. Heerschap, and W. P. J. Leenders, Antiangiogenic compounds interfere with chemotherapy of brain tumors due to vessel normalization. *Molecular Cancer Therapeutics* **7** (2008), No. 1, 71–78.
6. P. G. Corrie, Cytotoxic chemotherapy: clinical aspects. *Medicine* **36** (2008), No. 1, 24–28.
7. M. Curtarello, E. Zulato, G. Nardo, S. Valtorta, G. Guzzo, E. Rossi, G. Esposito, A. Msaki, A. Pasto, A. Rasola, L. Persano, F. Ciccarese, R. Bertorelle, S. Todde, M. Plebani, H. Schroer, S. Walenta, W. Mueller-Klieser, A. Amadori, R. M. Moresco, and S. Indraccolo. VEGF-targeted therapy stably modulates the glycolytic phenotype of tumor cells. *Cancer Research* **75** (2015), No. 1, 120–133.
8. P. V. Dickson, J. B. Hamner, T. L. Sims, C. H. Fraga, C. Y. C. Ng, S. Rajasekeran, N. L. Hagedorn, M. B. McCarville, C. F. Stewart, and A. M. Davidoff, Bevacizumab-induced transient remodelling of the vasculature in neuroblastoma xenografts results in improved delivery and ef-

ficacy of systemically administered chemotherapy. *Clinical Cancer Research* **13** (2007), No. 13, 3942–3950.

9. R. P. M. Dings, M. Loren, H. Heun, E. McNiel, A. W. Griffioen, K. H. Mayo, and R. J. Griffin, Scheduling of radiation with angiogenesis inhibitors anginex and Avastin improves therapeutic outcome via vessel normalization. *Clinical Cancer Research* **13** (2007), No. 11, 3395–3402.
10. A. W. El-Kareh and T. W. Secomb, A theoretical model for intraperitoneal delivery of cisplatin and the effect of hyperthermia on drug penetration distance. *Neoplasia* **6** (2004), No. 2, 117–127.
11. J. Folkman, Tumor angiogenesis: therapeutic implications. *New England J. Medicine* **285** (1971), No. 21, 1182–1186.
12. Genentech Inc, Avastin full Prescribing Information. https://www.gene.com/download/pdf/avastin_prescribing.pdf, 2017-04-13.
13. M.G. Ghosn, V.V. Tuchin, K.V. Larin, Depth-resolved monitoring of glucose diffusion in tissues by using optical coherence tomography. *Optics Letters* **31** (2006), No. 15, 2314–2316.
14. A. Giese, R. Bjerkvig, M. E. Berens, and M. Westphal, Cost of migration: invasion of malignant gliomas and implications for treatment. *J. Clinical Oncology* **21** (2003), No. 8, 1624–1636.
15. R. Grossman, H. Brastianos, J.O. Blakeley, A. Mangraviti, B. Lal, P. Zadnik, L. Hwang, R. T. Wicks, R. C. Goodwin, H. Brem, and B. Tyleret, Combination of anti-VEGF therapy and temozolomide in two experimental human glioma models. *J. Neuro-Oncology* **116** (2014), No. 1, 59–65.
16. D. Hanahan and R. A. Weinberg, Hallmarks of cancer: the next generation. *Cell* **144** (2011), No. 5, 646–674.
17. J. Holash, P. C. Maisonpierre, D. Compton, P. Boland, C. R. Alexander, D. Zagzag, G. D. Yancopoulos, and S. J. Wiegand, Vessel cooption, regression, and growth in tumors mediated by angiopoietins and VEGF. *Science* **284** (1999), No. 5422, 1994–1998.
18. R. K. Jain, Normalizing tumor vasculature with anti-angiogenic therapy: a new paradigm for combination therapy. *Nature Medicine* **7** (2001), No. 9, 987.
19. R. S. Kerbel and A. K. Barton, The anti-angiogenic basis of metronomic chemotherapy. *Nature Reviews Cancer* **4** (2004), No. 6, 423–436.
20. K. J. Kim, B. Li, J. Winer, M. Armanini, N. Gillett, H. S. Phillips, and N. Ferrara, Inhibition of vascular endothelial growth factor-induced angiogenesis suppresses tumour growth in vivo. *Letters to Nature* **362** (1993), 841–844.
21. Y. C. Kim, H. E. Grossniklaus, H. F. Edelhauser, and M. R. Prausnitz, Intrastromal delivery of bevacizumab using microneedles to treat corneal neovascularization intrastromal delivery of bevacizumab. *Investigative Ophthalmology & Visual Science* **55** (2014), No. 11, 7376–7386.
22. J. Kleinheinz, S. Jung, K. Wermker, C. Fischer, and U. Joos, Release kinetics of VEGF165 from a collagen matrix and structural matrix changes in a circulation model. *Head & Face Medicine* **6** (2010), No. 1, 17.
23. A. V. Kolobov, V. V. Gubernov, and M. B. Kuznetsov, The study of antitumor efficacy of bevacizumab antiangiogenic therapy using a mathematical model. *Russ. J. Numer. Anal. Math. Modelling* **30** (2015), No. 5, 289–297.
24. J. R. Levick, *An Introduction to Cardiovascular Physiology*. Butterworth–Heinemann, 2013.
25. J. Ma, S. Pulfer, S. Li, J. Chu, K. Reed, and J. M. Gallo, Pharmacodynamic-mediated reduction of temozolomide tumor concentrations by the angiogenesis inhibitor TNP-470. *Cancer Research* **61** (2001), No. 14, 5491–5498.
26. F. Milde, M. Bergdorf, and P. Koumoutsakos, A hybrid model for three-dimensional simulations of sprouting angiogenesis. *Biophysical J.* **95** (2008), No. 7, 3146–3160.

27. Y. Miyagi, K. Fujiwara, J. Kigawa, H. Itamochi, S. Nagao, E. Aotani, N. Terakawa, and I. Kohno, Intraperitoneal carboplatin infusion may be a pharmacologically more reasonable route than intravenous administration as a systemic chemotherapy. A comparative pharmacokinetic analysis of platinum using a new mathematical model after intraperitoneal vs. intravenous infusion of carboplatin-a Sankai Gynecology Study Group (SGSG) study. *Gynecologic Oncology* **99** (2005), No. 3, 591–596.

28. A. L. Myers, R. F. Williams, C.Y. Ng, J. E. Hartwich, and A. M. Davidoff, Bevacizumab-induced tumor vessel remodelling in rhabdomyosarcoma xenografts increases the effectiveness of adjuvant ionizing radiation. *J. Pediatric Surgery* **45** (2010), No. 6, 1080–1085.

29. C. S. Ng, C. Charnsangavej, W. Wei, and J. C. Yao, Perfusion CT findings in patients with metastatic carcinoid tumors undergoing bevacizumab and interferon therapy. *American J. Roentgenology* **196** (2011), No. 3, 569–576.

30. N. Papadopoulos, J. Martin, Q. Ruan, A. Rafique, M. P. Rosconi, E. Shi, E. A. Pyles, G. D. Yancopoulos, N. Stahl, and S. J. Wiegand, Binding and neutralization of vascular endothelial growth factor (VEGF) and related ligands by VEGF Trap, ranibizumab and bevacizumab. *Angiogenesis* **15** (2012), No. 2, 171–185.

31. S. Payne and D. Miles, *Mechanisms of Anticancer Drugs*, CRC press, 2008.

32. O. N. Pyaskovskaya, D. L. Kolesnik, A. V. Kolobov, S. I. Vovyanko, and G. I. Solyanik, Analysis of growth kinetics and proliferative heterogeneity of lewis lung carcinoma cells growing as unfed culture. *Exp. Oncol.* **30** (2008), No. 4, 269–275.

33. R. F. Schmidt and G. Thews, *Human Physiology*. Springer, Berlin–Heidelberg–New York, 1983.

34. M. Sooriyaarachchi, N. Aru, and G. Jurgen, Comparative hydrolysis and plasma protein binding of cis-platin and carboplatin in human plasma in vitro. *Metallomics* **3** (2011), No. 1, 49–55.

35. T. Sugiyama, M. Mizuno, Y. Aoki, M. Sakurai, T. Nishikawa, E. Ueda, K. Tajima, and N. Takeshima, A single-arm study evaluating bevacizumab, cisplatin, and paclitaxel followed by single-agent bevacizumab in Japanese patients with advanced cervical cancer. *Japanese J. Clinical Oncology*, (2016).

36. S. Urien and F. Lokiec, Population pharmacokinetics of total and unbound plasma cisplatin in adult patients. *British J. Clinical Pharmacology* **57** (2004), No. 6, 756–763.

37. A. A. M. Van der Veldt, M. Lubberink, I. Bahce, M. Walraven, M. P. de Boer, H. N. J. M. Greuter, N. H. Hendrikse, J. Eriksson, A. D. Windhorst, P. E. Postmus, H. M. Verheul, E. H. Serne, A. A. Lammertsma, and E. F. Smit, Rapid decrease in delivery of chemotherapy to tumors after anti-VEGF therapy: implications for scheduling of anti-angiogenic drugs. *Cancer Cell* **21** (2012), No. 1, 82–91.

38. H. Wang, H. Zhu, L. Kong, and J. Yu, Efficacy of cisplatin/pemetrexed with bevacizumab to treat advanced lung adenocarcinoma with different drive genes: case report and literature review. *OncoTargets Therapy* **9** (2016), 4639.